

## CONDUCTIVE MEMBRANES OBTAINED FROM COMB-TYPE FLUOROORGANOSILOXANES AND FLUOROORGANIC SALTS

**Tamara Tatrishvili<sup>1,2,✉</sup>, Tinatini Bukiashvili<sup>2,3</sup>, Nikoloz Kvinkadze<sup>1,2</sup>,  
Nana Pirtskheliani<sup>2,4</sup>, Tamar Makharadze<sup>2,3</sup>**

<sup>1</sup> Ivane Javakhishvili' Tbilisi State University, Department of Macromolecular Chemistry. 1 I. Chavchavadze Ave., Tbilisi 0179, Georgia

<sup>2</sup> Institute of Macromolecular Chemistry and Polymeric Materials, Ivane Javakhishvili Tbilisi State University, 13 I. Chavchavadze Ave, Tbilisi 0179, Georgia

<sup>3</sup> Vladimir Chavchanidze Institute of Cybernetics of the Georgian Technical University, 5 Z. Andjzaparidze St., Tbilisi 0186, Georgia

<sup>4</sup> Sokhumi State University, Faculty of Natural Sciences, Mathematics, Technologies and Pharmacy, 61 Politkovskaya St., Tbilisi 0186, Georgia

✉ [tamar.tatrishvili@tsu.ge](mailto:tamar.tatrishvili@tsu.ge)

© Tatrishvili T., Bukiashvili N., Kvinkadze N., Pirtskheliani N., Makharadze T., 2026

<https://doi.org/10.23939/chcht20.01.081>

**Abstract.** In this study, the hydrosilylation reaction of tetrahydrotetramethylcyclotetrasiloxane with allyl trifluoroacetate proceeded in the presence of catalysts (platinum, hydrochloric acid, Karstedt's catalysts, and Pt/C (10%)) at 323K was investigated. The expected D<sup>4</sup>R adduct was obtained. The D<sup>4</sup>R sample was analyzed by FTIR, <sup>1</sup>H, <sup>13</sup>C, and <sup>29</sup>Si NMR spectroscopy. A polymerization reaction of D<sup>4</sup>R-type fluoroorganocyclotetrasiloxane was carried out in the presence of a tetramethylammonium fluoride catalyst. The resultant reaction produced comb-type fluoro-organosiloxanes. Sol-gel reactions of fluoro organosiloxanes doped with lithium trifluoromethylsulfonate (triflate) or lithium bis(trifluoromethanesulfonyl)imide and tetraethoxysilane have been the subject of study, and solid polymer electrolyte membranes have been obtained. The ionic conductivities of these membranes have been determined using the technique of electrical impedance spectroscopy. It has been found that the electric conductivity of the polymer electrolyte membranes at room temperature changes in the range from 7.8x10<sup>-7</sup> to 3.2x10<sup>-6</sup> S/cm. This compound is an interesting product because, in addition to ester groups, it also contains fluorine host donor groups and, via sol-gel reactions, directly gives us thin films.

**Keywords:** hydrosilylation, sol-gel reactions, spectroscopy, polymer electrolyte membranes, ionic conductivity.

## Introduction

Polymer electrolytes (PEs) play an important role in electrochemical devices such as batteries and fuel cells. To achieve optimal performance, the PEs must maintain a high

ionic conductivity and mechanical stability at both high and low relative humidity. PEs also need to have excellent chemical stability for long product life and robustness.<sup>1-3</sup>

According to the prevailing theory, ionic conduction in any polymer electrolyte is facilitated by the large-scale segmental motion of the polymer backbone and primarily occurs in the amorphous regions of the polymer electrolyte. Crystallinity restricts polymer backbone segmental motion and significantly reduces conductivity. Consequently, polymer electrolytes with high conductivity at room temperature have been sought through polymers that have highly flexible backbones and have largely amorphous morphology. The interest in polymer electrolytes is increasing because of potential applications of solid electrolytes in high-energy-density solid-state batteries, gas sensors, and electrochromic windows.

An electric conductivity of 10<sup>-3</sup> S/cm is commonly regarded as a necessary minimum value for practical applications in batteries.<sup>4</sup> Polyethene oxide (PEO)-based systems are particularly thoroughly investigated. They reach room temperature conductivities of 10<sup>-7</sup> S/cm in some cross-linked salts in polymer systems based on amorphous PEO-polypropylene oxide copolymers. However, conductivity with such a value is unfortunately insufficient; it results from the semi-crystalline character of the polymer as well as from an increase in the glass transition temperature region of the system. It is widely accepted that for amorphous polymers with low glass transition temperature T<sub>g</sub> regions and high segmental mobility, the presence of halogens, especially fluorine groups, is important for achieving high ionic conductivities. Formation of the grid-like structures improves the mechanical properties of polymeric electrolytes.<sup>5-7</sup>

It is also well established that coordination of lithium ions takes place predominantly in the amorphous domains. Literature shows that PEO-based amorphous electrolytes can be obtained by the synthesis of comb-like polymers, namely by attaching short ethylene oxide unit sequences to existing amorphous polymer backbones.

The properties of organosilicon polymers depend on the structure of macromolecular chains and the nature of organic groups surrounding the silicon atoms.<sup>6</sup> Comb-type copolymers contain organic substituent groups of various sizes and natures bonded to hydrophobic methylsiloxane matrices. A wide range of variation of these substituent groups is possible. Some organosilicon copolymers contain donor groups and exhibit complexing properties.<sup>8-10</sup> A variety of organic donor groups can be bound to the silicon, including fluorine host groups in the side chain of the siloxane matrix, which gives us the possibility to change the ion-conducting properties of polymer electrolyte membranes.

Our work has several stages: 1) synthesis of  $D_4^R$ -type methylorganocyclotetra-siloxane with propyl-2,2,2-trifluoroacetate side group at silicon atoms; 2) determination of their structure by FTIR and NMR spectroscopy; 3) investigation of polymerization reaction of  $D_4^R$ -type fluoroorganocyclotetrasiloxane in the presence of catalyst tetramethylammonium fluoride and obtaining of comb type methylsiloxane polymers; 4) obtaining solid polymer electrolyte membranes via sol-gel reactions of such comb-type polymers doped with lithium trifluoromethyl-sulfonate (triflate) or lithium bis(trifluoromethanesulfonyl)imide and tetraethoxysilane; 5) determination of ionic conductivity of those membranes via electrical impedance spectroscopy.

## 2. Experimental

### 2.1. Materials

All synthetic procedures were performed under a dry dinitrogen gas atmosphere via standard vacuum line Schlenk techniques. Before use, solvents underwent degassing and purification using well-established procedures in the literature: toluene, hexane, and tetrahydrofuran were distilled via sodium/benzophenone ketyl. Aldrich reagents were used as received or distilled before use. 2,4,6,8-tetrahydro-2,4,6,8-tetramethylcyclotetrasiloxane ( $D_4^H$ ), vinyltriethoxysilane, Karstedt's catalyst – platinum (0)-1,3-divinyl-1,1,3,3-tetramethyldisiloxane complex (2% solution in xylene), platinum hydrochloric acid (Aldrich), Pt/C (10%), and lithium trifluoromethyl sulfonate (triflate) and lithium bis(trifluorosulphonyl)imide were purchased from Aldrich

and used as received. Toluene was dried and distilled from sodium under an atmosphere of dry nitrogen. Tetrahydrofuran (THF) was dried over and distilled from K–Na alloy under an atmosphere of dry nitrogen.<sup>11</sup>

### 2.2. Methods

**Fourier transform infrared spectroscopy (FTIR)** spectra studies were conducted on a Nicolet Nexus 470 machine with an MCTB detector.

**$^1H$ ,  $^{13}C$ , and  $^{29}Si$  NMR spectra** were recorded on a Bruker ARX400 NMR spectrometer at the 400 MHz operating frequency with  $CDCl_3$  as the solvent and an internal standard.

**Scanning electron microscopy (SEM) and Energy Dispersive Micro X-Ray Analysis (EDS)** were performed on SEM- Hitachi TM3030 Plus devices.

**Differential scanning calorimetric (DSC)** investigations were performed on a Netzsch DSC 200 F3 Maia apparatus. The measurement was carried out in an inert gas atmosphere under a nitrogen flow of 40 mL/min. The samples were heated from 173 K to 333 K.<sup>12</sup>

### 2.3. Hydrosilylation reaction of $D_4^H$ with allyl trifluoroacetate

$D_4^H$  2.6040 g (0.01083 mol) were transferred into a 100 mL flask under nitrogen using standard Schlenk techniques. High vacuum was applied to the flask for half an hour before the addition of 6.978 g (0.0453 mol) allyl trifluoroacetate in 5 mL dry toluene and Karstedt's precatalyst solution (20  $\mu$ L). The homogeneous mixture was degassed and placed into an oil bath, which was previously set to 60°C and the reaction continued at that temperature.

The reaction pathway was controlled by a decrease in the intensity of active  $\equiv Si-H$  groups.<sup>13</sup> After completion of the reaction, 0.1 wt. % of activated carbon was added and refluxed for 2 h for deactivation of the catalysts. All volatiles were removed by rotary evaporation at 50–60°C and further evacuated under high vacuum for 10 h to isolate 8.3 g (93.0%) of the colorless viscous compound I – 2,4,6,8-tetramethyl- 2,4,6,8-tetrapropyl trifluoroacetate) cyclotetrasiloxane ( $D_4^R$ ).

### 2.4. Ring-opening polymerisation of $D_4^R$

The 1.137 g (1.1498 mmol) of the  $D_4^R$  compound was transferred into a 50 mL flask under nitrogen. High vacuum was applied to the flask for half an hour. Afterwards, the compound was dissolved in 1.8 mL dry toluene. 0.01% of the total mass of tetramethylammonium fluoride was added. The mixture was degassed, placed in an oil bath that was previously set to 333 K, and

polymerised under nitrogen for 25 h. Then 7 mL of toluene was added to the reaction mixture, and the product was washed with water. The crude product was stirred with  $MgSO_4$  for 6 hours, filtered and evaporated. Then the product was precipitated at least three times into pentane to remove side products. Finally, all volatiles were removed under vacuum up to a constant mass. Thus, 1.0 g (85%) of colorless viscous polymer (II) with  $\eta_{sp} = 0.12$  has been isolated.

## 2.5. General Procedure for Preparation of Cross-Linked Polymer Electrolytes

We dissolved 1.0 g of the base compound in 4 mL of dry THF and thoroughly mixed it, then poured it onto a Teflon mold with a diameter of 4.0 cm. Then, a few drops of tetraethoxysilane and a catalytic amount of acid (one drop of 0.1N HCl solution in ethyl alcohol) were added to initiate the cross-linking process. The solvent was allowed to evaporate slowly overnight. Each membrane was allowed to evaporate slowly overnight. Finally, each membrane was dried in an oven at 343 K for 3 days and at 373 K for 1 h. This way we have obtained homogeneous and transparent films with an average thickness of 200  $\mu\text{m}$ . Our films were insoluble in water, while in THF, swelling was seen.<sup>14</sup>

## 2.6 AC Impedance Measurements

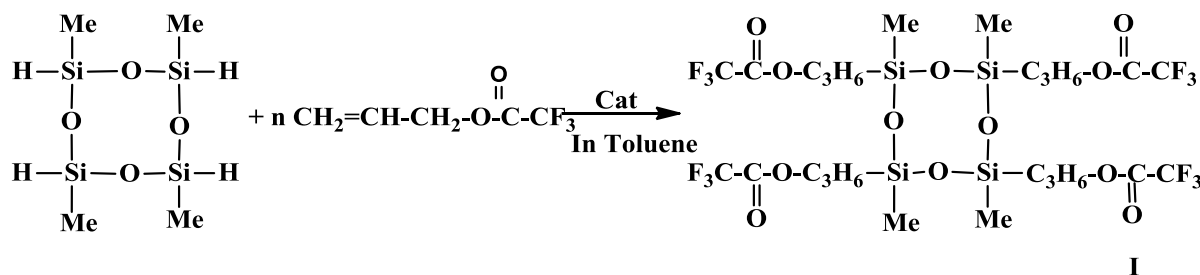
The total ionic conductivities of our samples were determined by placing an electrolyte disk between two 10 mm diameter brass electrodes. The electrode/electrolyte

assembly was secured in an appropriate constant volume support, which allowed reproducible measurements of conductivity in repeated heating-cooling cycles. The cell support was placed in an oven; the sample temperature was measured by a thermocouple positioned close to the electrolyte disk. The bulk conductivities of electrolytes during each heating cycle using the impedance techniques have been measured using a BM 507 Tesla impedance meter for frequencies from 50 Hz to 500 kHz over a temperature range from 30 to 90 °C.

## 3. Results and Discussion

For the synthesis of methylsiloxane polymers with propyl trifluoroacetate groups in the side chains, we have performed the reaction of the 2,4,6,8-tetrahydro compound in toluene solution. Under these conditions, the hydrosilylation reaction of  $D_4^H$  with allyl trifluoroacetate proceeds vigorously in the first 3-7 minutes.

We are interested in mitigating side reactions as well as in creating fully substituted cyclotetrasiloxanes. Therefore, we have investigated the temperature range. During the hydride addition reaction, changes in concentration of active  $\equiv\text{Si}-\text{H}$  bonds with time are seen in reactions of  $D_4^H$  with allyl trifluoroacetate in absolute toluene solution (50-60%) in the 303–323 K temperature range. The catalysts used show comparable reaction abilities. Apparently, in the hydrosilylation reactions, the Karstedt's catalysts used show higher reactivity than in the case of platinum on the carbon. The reaction proceeds according to the following Scheme 1:



Scheme 1. Hydrosilylation reaction of  $D_4^H$  with allyl trifluoroacetate

The organocyclotetrasiloxanes so obtained are transparent, viscous products; they are well soluble in ordinary organic solvents. The structures and compositions of those compounds were studied by determination of molecular masses,  $^1\text{H}$ ,  $^{13}\text{C}$ , and  $^{29}\text{Si}$  NMR spectroscopy. Some physical and chemical properties of organocyclotetrasiloxanes are presented in Table 1

In the FTIR spectra of compounds I (Fig. 1), one can observe absorption bands characteristic of asymmetric valence oscillation of linear  $\equiv\text{Si}-\text{O}-\text{Si}\equiv$  bonds at 1051  $\text{cm}^{-1}$ .

One can observe absorption bands at 795-800, 1188, 1265, 1735-1743, and 2800–3100  $\text{cm}^{-1}$ , characteristic of valence oscillation of  $\text{Si}-\text{CH}_3$ ,  $\text{CO}-\text{O}$ ,  $\text{Si}-\text{C}$ ,  $\text{C}=\text{O}$ , and  $\text{C}-\text{H}$  bonds, respectively. One can observe absorption bands for carbon-fluorine bonds.<sup>15,16</sup> The absorption bands characteristic of  $\text{Si}-\text{H}$  bonds disappear.

$^{29}\text{Si}$  NMR spectra of compound 1 (Fig. 2) showed resonance signals with chemical shifts = -19 ppm and -27 ppm characteristic for  $\text{RR}'\text{SiO}$  (D) units in a cyclic

fragment, signals  $\delta = -57.0$  ppm can be assigned to the D<sup>OR</sup> moieties. The triplet reflects stereochemical resolution due to isotactic and atactic resonance,

corresponding to the presence of RR'SiO (D), as well as a resonance signal with chemical shift  $\delta = -65$  ppm that can be assigned to T moieties in the triethoxysilyl group.

**Table 1.** Some physical chemical properties of organocyclotetrasiloxane

#	Compound	$n_D^{20}$	$d_4^{20}$	$M^*_{RD}$	$M^*$
I	$  \begin{array}{c}  \text{Me} \\    \\  \text{Si} - \text{O} \\    \\  \text{C}_3\text{H}_6 - \text{OCOCF}_3 \quad 4  \end{array}  $	1.39570	1.3457	<u>153.20</u> 152.72	<u>820</u> 856

\* numerator – calculated values; denominator – found values

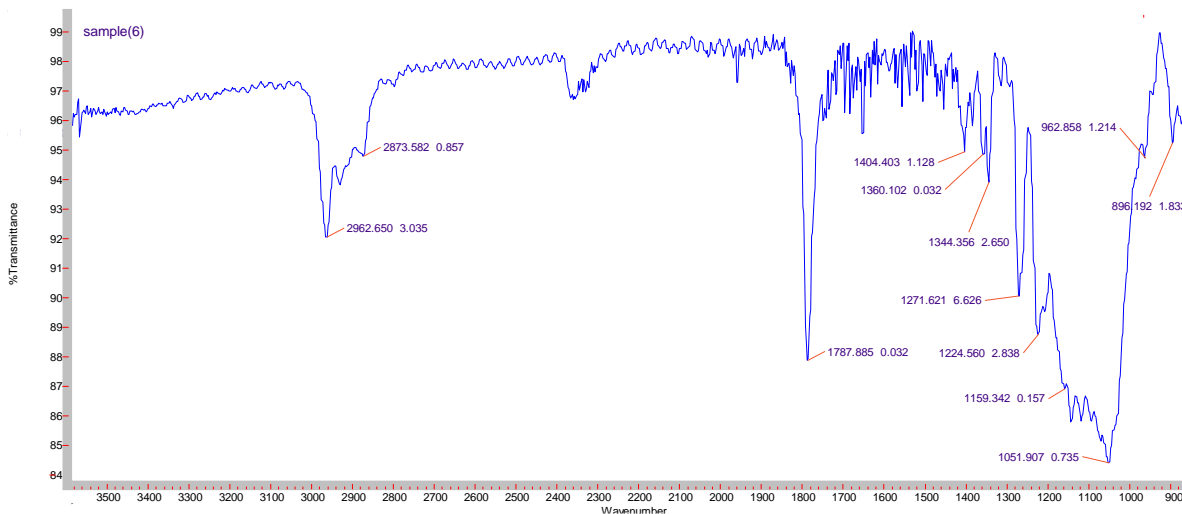


**Fig. 1.** FTIR spectra of compound I

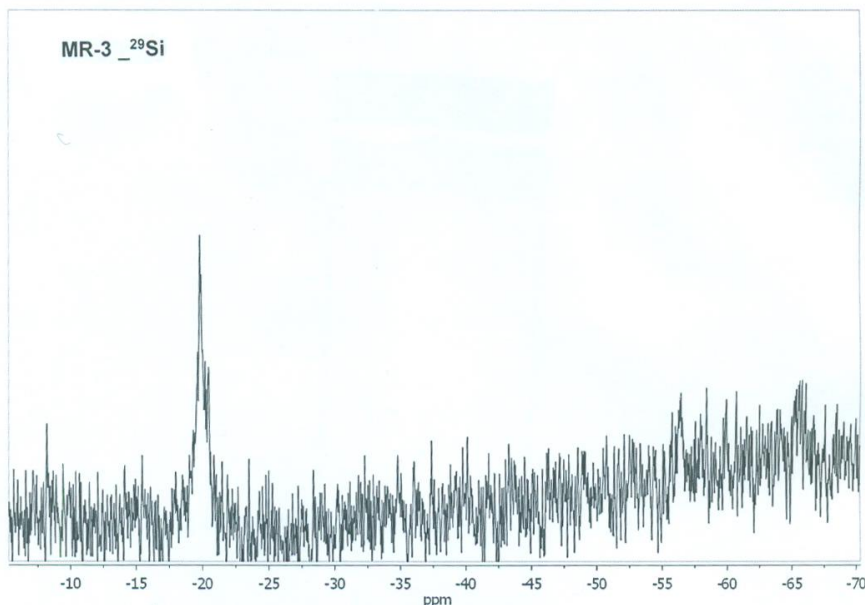


**Fig. 2.**  $^{29}\text{Si}$  NMR spectra of compound I

1. By  $^{29}\text{Si}$  NMR investigation, it was shown that in toluene solution proceeds only hydrosilylation reactions take place. In  $^{29}\text{Si}$  NMR spectra of compounds I, one can see a resonance signal with a chemical shift  $\delta = -20$  ppm, which corresponds to the presence of  $\text{RR}'\text{SiO}(\text{D})$  units.<sup>17</sup>

In  $^1\text{H}$  NMR spectra of compound I (Fig. 3), one can observe m-signals with a center of chemical shift at  $\delta$ =3.5 ppm for methylene protons in the fragment O-CH<sub>2</sub>-CH<sub>3</sub>. The signals at 0.6, 1.6 ppm for =CH-CH<sub>3</sub> and =CH-CH<sub>3</sub> (Markovnikov addition of vinyltriethoxysilane) overlap with the chemical shift of  $\alpha$ -addition of allyl groups.

In the  $^{13}\text{C}$ -NMR spectra of compound I (Fig. 4) one can observe signals characteristic for  $\equiv\text{Si}-\text{CH}_3$  groups with chemical shift at  $\delta\approx-0.2$  ppm and signals, for carbon atoms with chemical shifts at  $\delta\approx12.5, 16.1, 17.2, 68.1, 112.5, 157$  ppm corresponds to carbon atoms in the groups  $=\text{CH}-\text{CH}_3$ ,  $\text{SiCH}_2$ ,  $\text{SiCH}_2\text{CH}_2$ ,  $=\text{CH}-\text{CH}_3$ ,  $\text{SiCH}_2\text{CH}_2\text{CH}_2$ ,  $\text{CF}_3$  and  $\text{C}=\text{O}$  groups accordingly. Additionally, in the spectra one can observe chemical shifts for carbon atoms at 18.5 and 57.2 ppm, characteristic for carbon in the fragments  $\text{OCH}_2\text{CH}_3$  and  $\text{OCH}_2\text{CH}_3$ , respectively.<sup>18</sup>

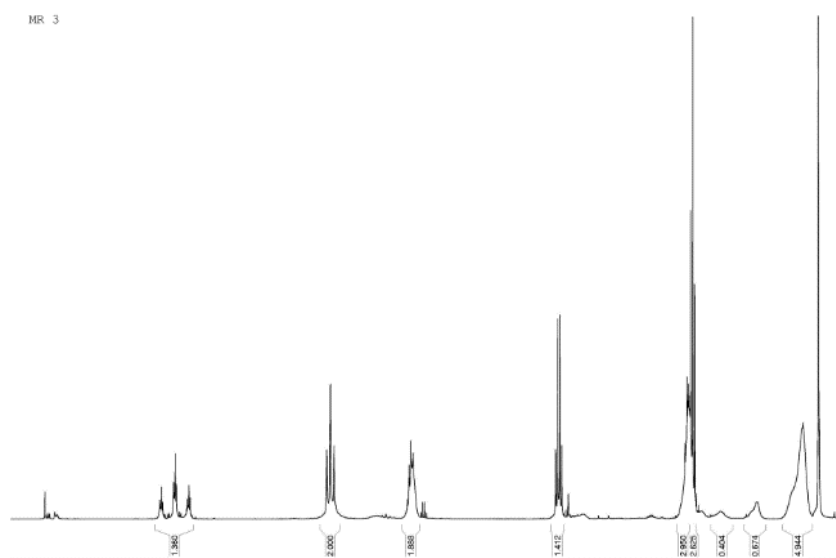


**Fig. 3.**  $^1\text{H}$  NMR spectra of compound I

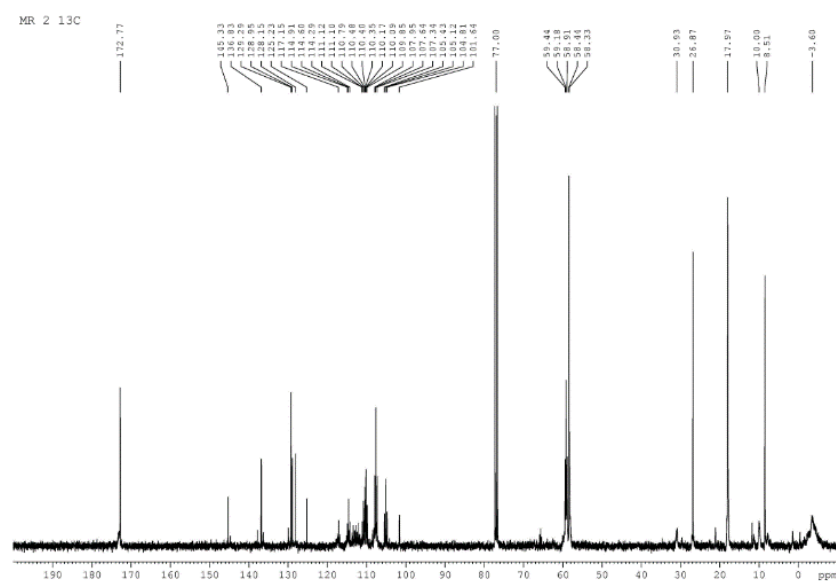


**Fig. 4**  $^{13}\text{C}$  NMR spectra of compound I

The hydrosilylation reaction of  $D_4^H$  with allyl trifluoroacetate proceeds (Fig. 5) very actively at a temperature range of 343–353 K, and the content of active Si-H groups after 10 minutes does not exceed 5–8%. The hydrosilylation reaction proceeds at approximately the same rate in the presence of platinum hydrochloric acid (0.1 M solution in THF) and Karstedt's catalyst ( $Pt_2(VinSiMe_2)_3$  in xylene), but with less activity in the presence of platinum on carbon. Figure 4 shows that the depth of the hydrosilylation reaction increases with temperature. The activity of catalysts for the hydrosilylation reaction of  $D_4^H$  with allyl trifluoroacetate was found to decrease in the following order: Karstedt's catalyst  $\approx H_2 PtCl_6 > Pt/C$ .

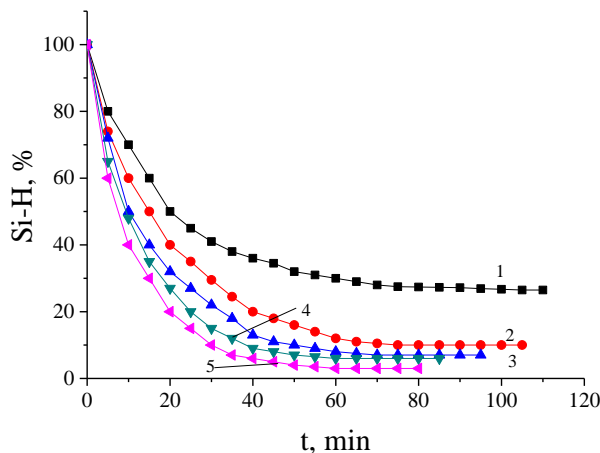
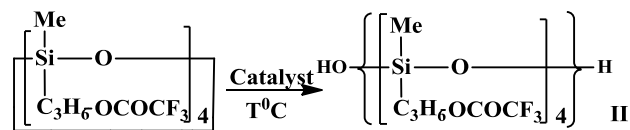


**Fig. 5.** Dependence of changes of concentration of active  $\equiv Si-H$  groups on the time, during hydrosilylation reaction of  $D_4^H$  with allyl trifluoroacetate, where curve 1 corresponds to the reaction, which was carried out at 323K- Pt/C, curve 2 – at 303 K, 3 – at 313K and curve 4 – at 323K – Karstedt's catalyst and curve 3 at 313K – platinum hydrochloric acid

From the dependence of the reverse reactant concentration on time, it was shown that, in the initial stages, hydrosilylation is a second-order reaction. The optimal conditions for the hydrosilylation reaction of  $D_4^H$  with allyl trifluoroacetate and vinyl triethoxysilane were determined to be a temperature of 323K, a dilute solution in a dry solvent (toluene), and Karstedt's catalyst.<sup>19</sup>

The polymerization reactions of  $D_4^H$  were carried out in the presence of tetramethylammonium fluoride, which was taken as 0.1 wt. % of the total mass of cyclic compound at 353 K.

The reaction proceeds according to the Scheme 2:



**Scheme 2.** Polymerization reaction of  $D_4^R$

The polymers so obtained were viscous, transparent systems well soluble in ordinary organic solvents, with  $\eta = 0.09 - 0.12$ . Their compositions and structures were determined via FTIR,  $^1H$ ,  $^{13}C$  and  $^{29}Si$  NMR spectroscopy.

In the FTIR spectra of polymer II (Figure 6), one can observe an absorption band for asymmetric valence oscillation characteristic of  $\equiv Si-O-Si=$  bonds in linear polydimethylsiloxane at  $1025\text{ cm}^{-1}$ . In the spectra, it is observed absorption bands at  $795-800$ ,  $1188$ ,  $1265$ ,  $1735-1743$ , and  $2800-3100\text{ cm}^{-1}$  which characterize valence oscillation of  $Si-CH_3$ ,  $CO-O$ ,  $\equiv Si-C=$ ,  $C=O$ , and  $\equiv C-H$  bonds, see Figures 9 and 10. In the spectra of the polymer also observe absorption bands at  $3200-3400\text{ cm}^{-1}$ , characterized by  $Si-OH$  bonds, which proves that polymerization proceeds via a ring-opening method.

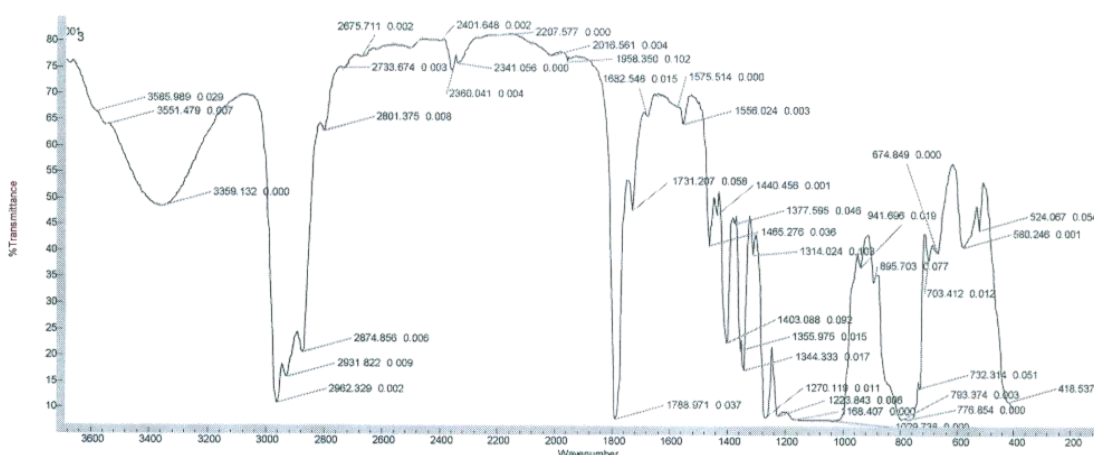
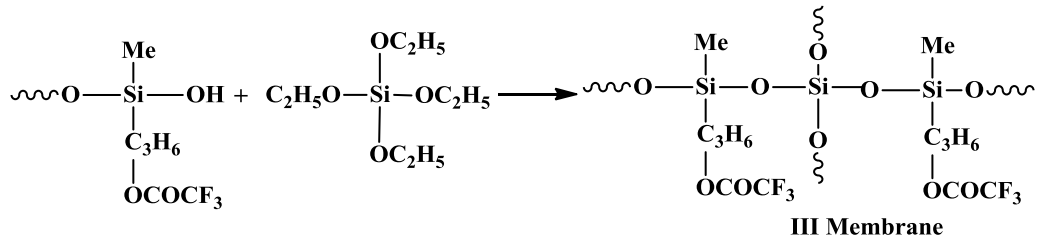


**Fig. 6.** FTIR spectra of polymer II

Based on polymer II, polymer electrolyte membranes have been obtained using triflate: III (1) – 5%; III (2) – 10%, III (3) – 15%; III (4) – 20%. Based on lithium bis (trifluorosulfonyl) imide, we have obtained PE



**Scheme 3.** Sol-gel processes for the preparation of Membrane III

The present study investigates the electrophysical properties and temperature-dependent conductivity characteristics of polyethylene (PE) membranes, focusing on the molecular and supramolecular structure of PE. The study utilised a range of electrophysical methods, including EPR, optical microscopy, and SEM, to achieve its objectives.

2. By wide-angle X-ray diffraction investigation (Fig. 7), it was shown that the obtained membranes are also amorphous systems. As it is seen from Figure 6, one can observe a maximum at the  $17.5 - 2 \text{ } \Theta^0$  region.

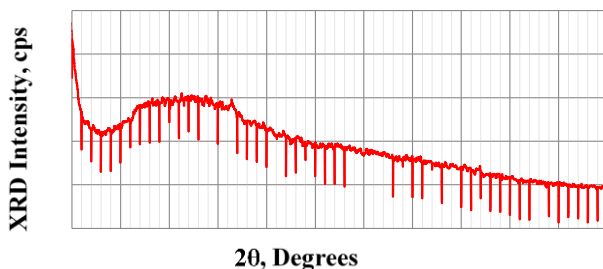


**Fig. 7.** Wide-angle X-Ray analysis III (2)

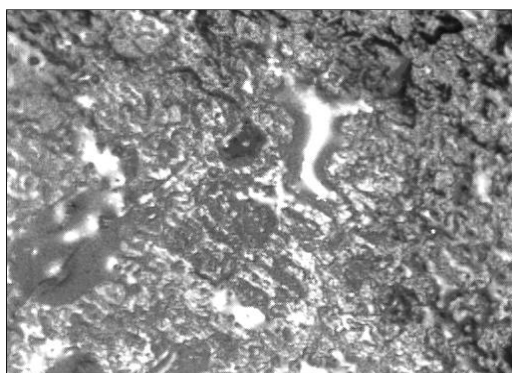
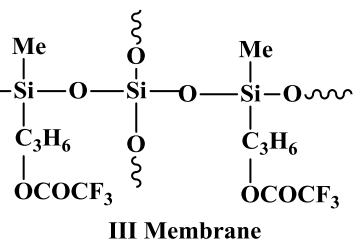


**Fig. 8.** Electron-microscopic images of membranes III (2) (10% - Lithium triflate) at 100 (1) and 200 (2) magnifications

membranes: III (5) – 5%; III (6) – 10%, III (7) – 15%; III (8) – 20%.

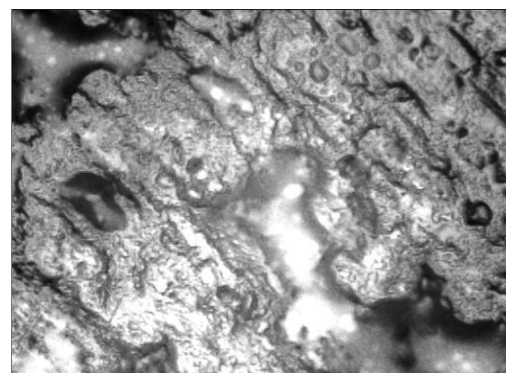
Sol-gel reaction of polymer II proceeds according to the Scheme 3:



3. The electronic-microscopic examination of NMM-800RF / TRF on polymer electrolyte membrane III (2) has been conducted. As shown in Fig. 8, the images are exposed to amorphous inserts of lithium salts that promote the durability of ions.

A differential scanning calorimetric investigation has been conducted on a sample of polymer electrolyte membrane III. As demonstrated in Fig. 9, the DSC curves illustrate that membrane III is distinguished by a lower glass transition temperature of  $-31.00^\circ\text{C}$ .<sup>20</sup>

The morphology of the surface of the membrane III (3) (15%  $-\text{CF}_3\text{SO}_3\text{Li}$  salt) has been examined via scanning electron microscopy and X-ray energy-dispersive microscopy. In Fig. 10, we show SEM micrographs of PE membranes III(3) at two different locations. The figure clearly shows a fairly smooth and uniform surface morphology. This morphology confirms the fully amorphous nature of the PE membranes and also the complete dissolution of the lithium salt, which agrees with the XRD results. The image shows the dispersion of the fillers; it also shows a small pore entrapping the ionic liquid, which allows fast ionic motions. The well-visible amorphous layers of lithium salts provide high ionic conductivity.<sup>21-29</sup>



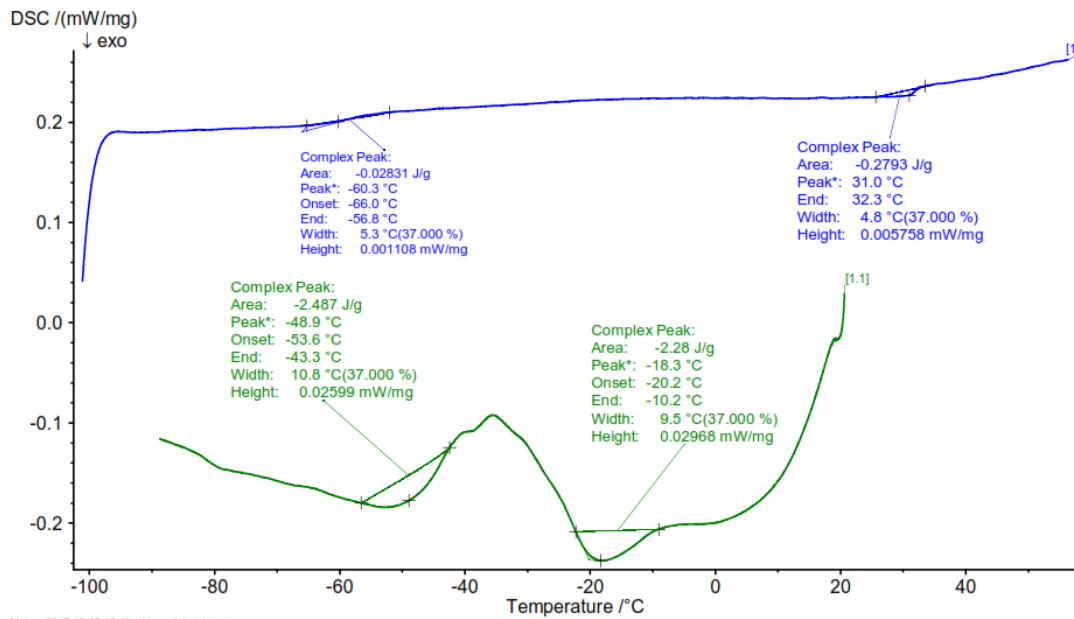


Fig. 9. DSC curves of the membrane III (4) (Lithium triflate 20%)

We show in Fig. 11 energy dispersive X-ray patterns of the polymer electrolyte membrane III (3). We can see a relatively homogeneous distribution of the lithium salt in the polymeric matrix.

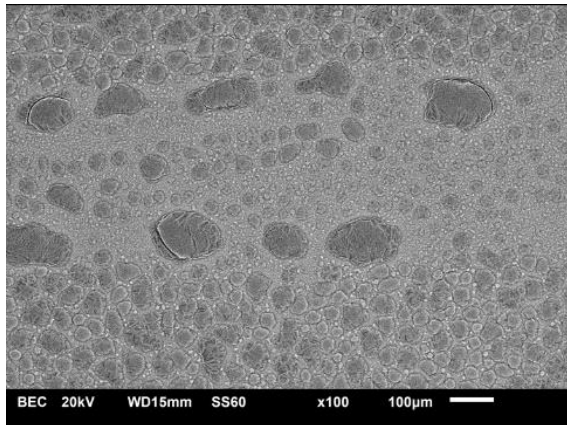


Fig. 10. SEM micrographs of membrane III (3) (15%  $-\text{CF}_3\text{SO}_3\text{Li}$  salt)

In Table 2, we provide values of the ionic conductivity of polymer electrolyte membranes III.<sup>30,31</sup>

Table 2. Initial ion conductivity of the polymer membranes III at room temperature

#	Salt (Wt.%)	$\sigma$ (25°C), S/cm
1	2	3
1	$\text{CF}_3\text{SO}_3\text{Li}$ (5)	$7.8 \times 10^{-7}$
2	$\text{CF}_3\text{SO}_3\text{Li}$ (10)	$8.5 \times 10^{-6}$

We have determined the specific volumetric electroconducting properties at room temperature, their temperature dependences, and also their voltamperic characteristics; see now Figs. 12-14.

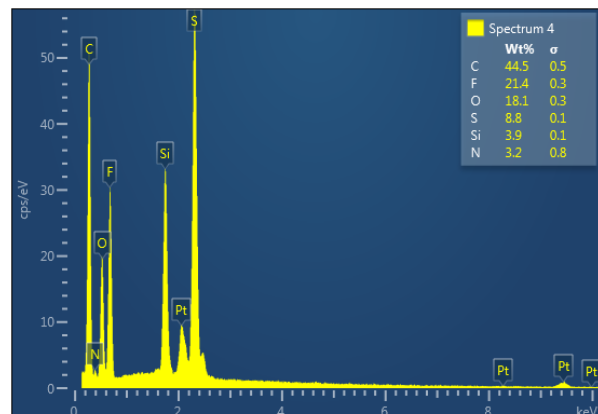


Fig. 11. Energy dispersive X-ray microanalysis of membrane III (3), spectrum 4

Continuation of Table 2.

1	2	3
3	$\text{CF}_3\text{SO}_3\text{Li}$ (15)	$7.2 \times 10^{-6}$
4	$\text{CF}_3\text{SO}_3\text{Li}$ (20)	$1.0 \times 10^{-6}$
5	$(\text{CF}_3\text{SO}_2)_2\text{NLi}$ (5)	$8.4 \times 10^{-7}$
6	$(\text{CF}_3\text{SO}_2)_2\text{NLi}$ (10)	$3.2 \times 10^{-6}$
7	$(\text{CF}_3\text{SO}_2)_2\text{NLi}$ (15)	$7.3 \times 10^{-6}$
8	$(\text{CF}_3\text{SO}_2)_2\text{NLi}$ (20)	$7.8 \times 10^{-7}$

From Table 2, we infer that the specific volumetric electrical conductivities of the membranes vary in the range from  $7.8 \cdot 10^{-7}$  to  $3.2 \cdot 10^{-6}$  S/cm. The most appropriate values of the conductivity are for the interval between 10 and 15 wt.%, while outside of that range, we see relatively low conductivity values. The

reasons for this are fairly low densities of ions (thus low conducting charge densities) from one side and, in accordance with a popular opinion, the creation of ionic pairs at relatively high concentrations of salts in the membranes because of the low mobility of the charges from the other side.

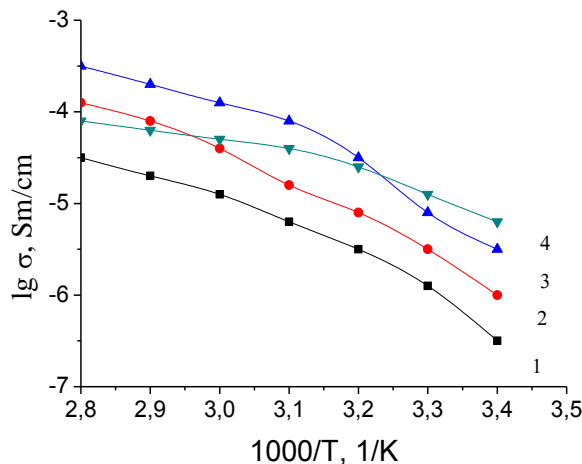


**Fig. 12.** Temperature dependence of specific electrical conductivity of membranes based on polymer II and triflate salt. Curve 1 corresponds to PE membrane III (1), 2 to III (2), 3 to III (3), and 4 to III (4)

We show in Fig. 14 the voltammograms of polymer electrolyte membranes with high values of ionic conductivity. We see that the ionic conductivity of the membranes is much higher than their specific conductivity. A convincing explanation of the mechanism of ionic conduction would require more experiments.

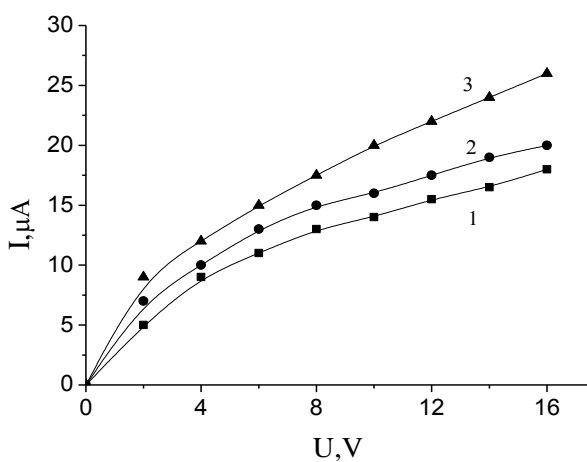


**Fig. 14.** Voltammograms of polymer electrolyte membranes. Curve 1 corresponds to membrane 1- III (2), curve 2 to III (2), and curve 3 to III (7)

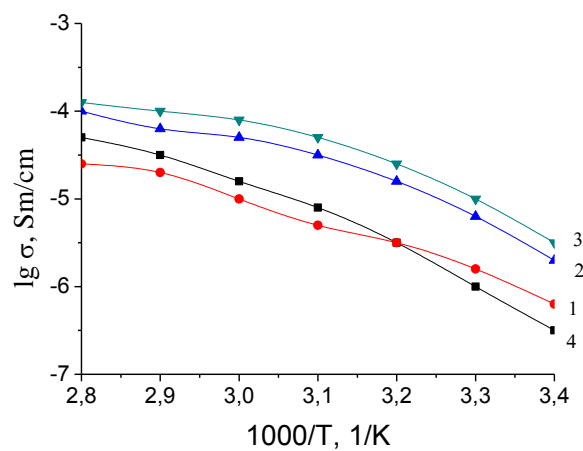


**Fig. 13.** Temperature dependence of specific electrical conductivity of membranes based on polymer II and lithium bis(trifluoromethanesulfonyl)imide salt. The curve 1 corresponds to PE membrane III (5), 2 to III (6), 3 to III (7), and 4 to III (8)

We have also created membranes containing  $\text{Al}_2\text{O}_3$ . It is known that even a small amount of this substance leads to an increase in the membrane conductivity to some extent. The conductivities of membranes containing this substance are presented in Table 3. The values in the brackets pertain to samples that do not contain  $\text{Al}_2\text{O}_3$ .

**Table 3.** Electrical conductivities of membranes

N	Membrane	Salt (Wt%)	$\text{Al}_2\text{O}_3$ , (Wt.%)	$\sigma$ (25°C), S/cm
1	III (2)	$\text{CF}_3\text{SO}_3\text{Li}$ (10)	5	$1.1 \times 10^{-5}$ ( $8.5 \times 10^{-6}$ )
2	III (2)	$\text{CF}_3\text{SO}_3\text{Li}$ (10)	10	$2.6 \times 10^{-5}$ ( $8.5 \times 10^{-6}$ )
3	III (7)	$(\text{CF}_3\text{SO}_2)_2\text{NLi}$ (15)	10	$9.8 \times 10^{-6}$ ( $7.3 \times 10^{-6}$ )

\*In the brackets, the numerical data of conductivities of the corresponding membranes without  $\text{Al}_2\text{O}_3$

#### 4. Conclusions

Hydrosilylation reaction of 2,4,6,8-tetrahydro-2,4,6,8-tetramethylcyclotetrasiloxane ( $\text{D}_4^{\text{H}}$ ) with allyl

trifluoroacetate, in the presence of platinum catalysts, has been studied, and expected adducts have been obtained.

By ring-opening copolymerization reaction of  $D_4^R$  in the presence of tetramethylammonium fluoride at 343 K, comb-type polymers have been obtained.

The structure and composition of the obtained  $D_4^R$  type compound (I) and polymer (II) have been determined via molecular mass determination, also by molecular refraction determination, FTIR,  $^1H$ ,  $^{13}C$ , and  $^{29}Si$  NMR spectral data.

We have studied the sol-gel reaction of polymer II doped with lithium trifluoromethanesulfonate (triflate) and lithium bis (trifluoromethanesulfonyl)imide; solid polymer electrolyte membranes have thus been obtained. Via electrical impedance spectroscopy, ion-conductivities of solid polymer electrolyte membranes depending on the salt concentration have been determined in the range from  $8.4 \times 10^{-7}$  to  $3.2 \times 10^{-6}$  S/cm. Inclusion of corundum ( $Al_2O_3$ ) at concentrations of 5-10% leads to an increase in the membrane ionic conductivity to some extent.

## References

- [1] Muldoon, J.; Bucur, C.B.; Boaretto, N.; Gregory, Th.; di Noto, V. Polymers: Opening Doors to Future Batteries. *Polym. Rev.* **2015**, *58*, 208–246. <https://doi.org/10.1080/15583724.2015.1011966>
- [2] Sun, Ch.; Liu, J.; Gong, Yu.; Wilkinson, D.P.; Zhang, J. Recent Advances in All-Solid-State Rechargeable Lithium Batteries. *Nano Energy* **2017**, *33*, 363–386. <https://doi.org/10.1016/j.nanoen.2017.01.028>
- [3] Goodenough, J.B.; Park, K-S. The Li-Ion Rechargeable Battery: A Perspective. *J. Am. Chem. Soc.* **2013**, *135*, 1167–1176. <https://doi.org/10.1021/ja3091438>
- [4] Armand, M.B.; Bruce, P.G.; Forsyth, M.; Scrosati, B.; Wieszorek, W. Polymer electrolytes. In *Energy Materials*; Bruce, D.W.; O'Hare, D.; Walton, R.I., Eds.; John Wiley & Sons, Ltd., 2011; pp. 1–27. <https://doi.org/10.1002/9780470977798.ch1>
- [5] Grünebaum, M.; Hiller, M.; Jankowsky, S.; Pohl, S.E.; Schürmann, Th.; Vettikuzha, P.; Gentschev, A-Ch.; Stolina, R.; Müller, R.; Wiemhöfer, H-D. Synthesis and Electrochemistry of Polymer-Based Electrolytes or Lithium Batteries. *Prog. Solid State Chem.* **2014**, *42*, 85–105. <https://doi.org/10.1016/j.progsolidstchem.2014.04.004>
- [6] Yue, L.; Ma, J.; Zhang, J.; Zhao, J.; Dong, S.; Liu, Z.; Cui, G.; Chen, L. All Solid-State Polymer Electrolytes for High-Performance Lithium-Ion Batteries. *Energy Storage Mater.* **2016**, *15*, 139–164. <https://doi.org/10.1016/j.ensm.2016.07.003>
- [7] Kim, D-G.; Shim, J.; Lee, J.H.; Kwon, S-J.; Baik, J-H.; Lee, J-C. Preparation of Solid-State Composite Electrolytes Based on Organic/Inorganic Hybrid Star-Shaped Polymer and PEG-Functionalized POSS for All-Solid-State Lithium Battery Applications. *Polymer* **2013**, *54*, 5812–5820. <https://doi.org/10.1016/j.polymer.2013.08.049>
- [8] Ben Youcef, H.; Garcia-Calvo, O.; Lago, N.; Devaraj, Sh.; Armand, M. Cross-Linked Solid Polymer Electrolyte for All-Solid-State Rechargeable Lithium Batteries. *Electrochim. Acta* **2015**, *220*, 587–594. <https://doi.org/10.1016/j.electacta.2016.10.122>
- [9] Liu, T.-M.; Saikia, D.; Ho, S.-Y.; Chen, M.-Ch.; Kao, H.-M. High Ion-Conducting Solid Polymer Electrolytes Based on Blending Hybrids Derived from Monoamine and Diamine Polyethers for Lithium Solid-State Batteries. *RSC Adv.* **2017**, *7*, 20373–20383. <https://doi.org/10.1039/C7RA01542A>
- [10] Boaretto, N.; Joost, Ch.; Seyfried, M.; Vezzù, V.K.; Di Noto, Di. Conductivity and Properties of Polysiloxane-Polyether Cluster-LiTFSI Networks as Hybrid Polymer Electrolytes. *J. Power Sources* **2016**, *325*, 427–437. <https://doi.org/10.1016/j.jpowsour.2016.06.034>
- [11] Mukbaniani, O.; Zaikov, G.; Tatrishvili, T. Organosilicon Copolymers with Monocyclic Fragments in the Main Dimethylsiloxane Backbone. A Review. *Oxidation Communications* **2006**, *29*, 776–792.
- [12] Mukbaniani, O.; Tatrishvili, T.; Pachulia, Z.; Londaridze, L.; Pirtskheliani, N. Quantum-Chemical Modelling of Hydrosilylation Reaction of Triethoxysilane to Divinylbenzene. *Chem. Chem. Technol.* **2023**, *16*, 499–506. <https://doi.org/10.23939/chcht16.04.499>
- [13] Mukbaniani, O.; Zaikov, G.; Tatrishvili, T.; Titvinidze, G.; Phatsatsia, S. Synthesis of New Methylsiloxane Oligomers with Pendant Trialkoxysilylethyl Groups for Preparation of Silicon Hard Coatings. *Macromol. Symp.* **2007**, *247*, 393–404. <https://doi.org/10.1002/masy.200750146>
- [14] Röchow, E.T.; Coeler, M.; Pospiech, D.; Kobsch, O.; Mechtaeva, E.; Vogel, R.; Voit, B.; Nikolowski, K.; Wolter, M. In Situ Preparation of Crosslinked Polymer Electrolytes for Lithium Ion Batteries: A Comparison of Monomer Systems. *Polymers* **2020**, *12*, 1707. <https://doi.org/10.3390/polym12081707>
- [15] Socrates, G. *Socrates Infrared and Raman characteristic group frequencies: tables and charts*; John Wiley and Sons, 2001.
- [16] Stuart, B.H. *Infrared Spectroscopy: Fundamentals and Applications*; John Wiley and Sons, 2004. <https://doi.org/10.1002/0470011149>
- [17] Bursch, M.; Gasevic, Th.; Stückrath, Ju.B.; Grimme, S. Comprehensive Benchmark Study on the Calculation of  $^{29}Si$  NMR Chemical Shifts. *Inorg. Chem.* **2021**, *60*, 272–285. <https://doi.org/10.1021/acs.inorgchem.0c02907>
- [18] Gunawan, R.; Nandiyanto, A.B.D. How to Read and Interpret  $^1H$ -NMR and  $^{13}C$ -NMR Spectrums. *Indones. J. Sci. Technol.* **2021**, *6*, 267–298.
- [19] Mukbaniani, O.; Tatrishvili, T.; Mukbaniani, N. Comb-Type Methylsiloxane Copolymers with Diorganosilylene Fragments as a Lateral Group. *J. Appl. Polym.* **2007**, *104*, 2161–2167. <https://doi.org/10.1002/app.24474>
- [20] Lin, C.; Kao, H.; Wu, R.; Kuo, P. Multinuclear Solid-State NMR, DSC, and Conductivity Studies of Solid Polymer Electrolytes Based on Polyurethane/Poly(dimethylsiloxane) Segmented Copolymers. *Macromolecules* **2002**, *35*, 3083–3096. <https://doi.org/10.1021/ma012012q>
- [21] Petriashvili, G.; Chanishvili, A.; Ponjavidze, N.; Chubinidze, K.; Tatrishvili, T.; Kalandia, E.; Petriashvili, A.; Makharadze, T. Crystal Smectic G Phase Retarder for the Real-Time Spatial-Temporal Modulation of Optical Information. *Chem. Chem. Technol.* **2023**, *17*, 758–765. <https://doi.org/10.23939/chcht17.04.758>
- [22] Tatrishvili, T.; Mukbaniani, O.; Kvinkadze, N.; Bukiashvili, T.; Pirtskheliani, N.; Chikhladze, Sh. Wood Flour Composites: Obtaining and Research. *Chem. Chem. Technol.* **2024**, *18*, 567–579. <https://doi.org/10.23939/chcht18.04.567>
- [23] Tatrishvili, T.; Mukbaniani, O.; Kvinkadze, N.; Chikhladze, Sh.; Bukiashvili, T.; Petriashvili, G.; Pirtskheliani, N.; Makharadze, T. <https://doi.org/10.23939/chcht18.04.567>

Novel Composites Based on a Natural Raw Material and Silylated Polystyrene. *Chem. Chem. Technol.* **2024**, *18*, 580–591. <https://doi.org/10.23939/chcht18.04.580>

[24] Petriashvili, G.; Chubinidze, K.; Tatrishvili, T.; Kalandia, E.; Petriashvili, A.; Chubinidze, M. Light-Stimulated Lowering of Glucose Concentration in a Dextrose Solution Mediated by Merocyanine Molecules. *MatTech* **2023**, *57*, 119–124. <https://doi.org/10.17222/mit.2022.639>

[25] Mukbaniani, O.; Aneli, J.; Tatrishvili, T. Biocomposites-Environmental and Biomedical Applications; Apple Academic Press, 2023.

[26] Petriashvili, G.; Sulaberidze, T.; Tavkhelidze, D.; Janikashvili, M.; Ponjavidze, N.; Chanishvili, A.; Chubinidze, K.; Tatrishvili, T.; Makharadze, T.; Kalandia, E.; *et al.* Cholesteric Liquid Crystal Mirror-Based Smart Window Controlled with Ambient Temperature. *Chem. Chem. Technol.* **2024**, *18*, 401–408. <https://doi.org/10.23939/chcht18.03.401>

[27] Bukić, T.; Utiashvili, M.; Tsiskarishvili, M.; Jalalishvili, S.; Gogolashvili, A.; Tatrishvili, T.; Petriashvili, G. Synthesis of Some Azo Dyes Based on 2,3,3-Trimethyl-3h-Indolenine. *Chem. Chem. Technol.* **2023**, *17*, 549–556. <https://doi.org/10.23939/chcht17.03.549>

[28] Mukbaniani, O.; Tatrishvili, T.; Titvinidze, G.; Mukbaniani, N. Formation of New Thermoreactive Polysiloxanes. *J. Appl. Polym. Sci.* **2007**, *104*, 2168–2173. <https://doi.org/10.1002/app.24740>

[29] Mukbaniani, O.; Zaikov, G.; Tatrishvili, T.; Titvinidze, G.; Mukbaniani, N. Methylsiloxane Oligomers with Oxyalkyl Fragments in the Side Chain. *Macromol. Symp.* **2007**, *247*, 364–370. <https://doi.org/10.1002/masy.200750142>

[30] Rossi, N.A.; West, R. Silicon-Containing Liquid Polymer Electrolytes for Application in Lithium-Ion Batteries. *Polym. Int.* **2009**, *58*, 267–272. <https://doi.org/10.1002/pi.2523>

[31] Snyder, J.F.; Ratner, M.A.; Shriver, D.F. Ion Conductivity of Comb Polysiloxane Polyelectrolytes Containing Oligoether and Perfluoroether Sidechains. *J. Electrochem. Soc.* **2003**, *150*, A1090–A1094. <https://doi.org/10.1149/1.1589759>

Received: June 12, 2025 / Revised: June 29, 2025 /

Accepted: September 05, 2025

## ПРОВІДНІ МЕМБРАНИ, ОТРИМАНІ З ФТОРОРГАНОСИЛОКСАНІВ ГРЕБЕНЕВОГО ТИПУ ТА ФТОРОРГАНІЧНИХ СОЛЕЙ

**Анотація.** У цій роботі було досліджено реакцію гідросиліювання тетрагідротетраметилциклотрасілоксану з алілтрифторацетатом у присутності катализаторів (платини, соляної кислоти, катализаторів Карстедта та Pt/C (10 %)) при температурі 323 К. Було отримано очікуваний аддукт  $D_4^R$ . Зразок  $D_4^R$  було проаналізовано за допомогою FTIR,  $^1H$ ,  $^{13}C$  та  $^{29}Si$  NMR спектроскопії. Реакцію полімеризації фторорганічного циклотрасілоксану типу  $D_4^R$  було проведено в присутності катализатора тетраметиламонію фториду. В результаті реакції утворилися гребінчасті фторорганічні силоксані. Були досліджені золь-гель реакції фторорганічних силоксанів, легованих трифторметилсульфонатом літію (трифлатом) або біс(трифторметансульфоніл)імідом літію та тетраетоксисиланом, і отримано тверді полімерні електролітні мембрани. Іонна провідність цих мембран була визначена за допомогою методу електроімпедансної спектроскопії. Було встановлено, що електропровідність полімерних електролітних мембран при кінній температурі змінюється в діапазоні від  $7,8 \times 10^{-7}$  до  $3,2 \times 10^{-6}$  См/см. Ця сполука є цікавим продуктом, оскільки, крім ефірних груп, вона також містить фторні донорні групи і за допомогою золь-гель реакції безпосередньо дає нам тонкі плівки.

**Ключові слова:** гідросиліювання, золь-гель реакції, спектроскопія, полімерні електролітні мембрани, іонна провідність.